

# Spectroscopic and electrical characterization of gettering effect in p- and n-type multi-crystalline silicon

M. Acciarri<sup>1</sup>, S. Binetti<sup>1</sup>, A. Le Donne<sup>1</sup>, S. Marchionna<sup>1</sup>, S. Pizzini<sup>1</sup>, J. Libal<sup>2</sup>, R. Kopecek<sup>2</sup>, I. Röver<sup>3</sup>, K. Wambach<sup>3</sup>

<sup>1</sup> Dept. of Material Science, Università di Milano-Bicocca, via Cozzi 53, I-20125 Milano, Italy

<sup>2</sup> University of Konstanz, Jakob-Burckhardt-Str. 29, D-78464 Konstanz, Germany

<sup>3</sup> Deutsche Solar, Alfred-Lange Str. 18, D-09599 Freiberg/Sachsen, Germany

**ABSTRACT:** The increase of the average lifetime in silicon multicrystalline wafers at the end of the cell fabrication process shows that, like in p-type materials, also in n-type materials the average quality can be improved by suitable gettering and passivation treatments. However, it was already reported that different parts of p-doped ingots react in different way to the gettering procedures. In this paper we report on the effect of the phosphorus (P)-gettering process (45 Ohm/sq P-diffusion) on n- and p-type mc Si in order to get more information about the physics of the gettering process in both materials. The detailed analysis of the electrical activity of microstructural defects shows that grain boundaries and precipitates are the more detrimental defects, even if they do not deteriorate the average good quality of the material and the final cell performance. No intragranular electrical active defects could be detected in the EBIC maps at room temperature. Finally, despite the formation of precipitates at grain boundaries, the average diffusion lengths in n-type samples are larger than in p-type samples prepared in similar conditions, confirming that n-type-Si is less sensitive to metallic impurities.

**Keywords:** gettering, multi-crystalline, defects

## 1 INTRODUCTION

The photovoltaic (PV) market has sustained important growth in the last decade. Annual production has increased at yearly rate of about 30%-40% while manufacturing cost has reduced enormously. In the last two years the PV industry has produced modules for over a gigawatt per year and used 45% of the total world production of high purity-polysilicon [1]. However, this rapid increase of the PV industry has created a shortage of silicon that will probably reduce the annual increase of this market.

Recently, n-type mc-Si has attracted attention as a partial or short term solution to the main current problem for the photovoltaic industry: the silicon supply. A partial solution not yet on the market is in fact the use of the n-doped silicon waste available from the semiconductor industry.

For this purpose, in the last three years different studies have been carried out on the properties of n-type mc-Si and on the development and optimisation of a solar cell process for n-type mc-Si [2, 3]. The first results on solar cells based on n-type material using industrial processes have already shown excellent efficiencies exceeding 17% in single crystal material [4, 5].

However, the evolution of the electrical and optical properties of the n-type mc-Si during the solar cell process is not yet completely understood. An in-depth study is necessary for further improved of the material quality by suitable gettering and passivation treatments [2, 6] like in p-type materials.

In this paper we report on the effect of the phosphorus (P)-gettering process (45 Ohm/sq P-diffusion) on n- and p-type mc Si in order to get more information about the efficiency of the gettering process in both materials.

## 2 EXPERIMENTAL DETAILS

Two Sb- and B- doped silicon ingots were grown in the same furnace and then cut in wafers having a

thickness ranging from 330 to 270  $\mu\text{m}$ . In this paper we concentrated our characterization on wafers coming from the middle part of the ingots. For the analysis couples of nearby wafers with the same morphology were selected. One wafer for each couple was submitted to the P-diffusion step, according to the following procedure:

- Saw damage removal: 20 minutes CP4-etch
- P-diffusion step: 45 Ohm/sq  $\text{POCl}_3$ -diffusion ( $T = 850^\circ\text{C}$  approx.)
- Removal of P-doped region: 30 minutes CP4-etch

Table I shows the features of the samples characterized in this work (i.e. ingot type, dopant, positions and codes).

All wafers were characterized before and after the P-diffusion step as it follows. Microwave-detected PhotoConductance Decay ( $\mu\text{W-PCD}$ ) spatially resolved lifetime maps were carried out with a Amecon Janus 300 Lifetime scanner. The Janus 300 uses a laser diode with  $\lambda = 908\text{ nm}$  for illumination to create the excess charge carriers. For all measurements the intensity of the laser has been chosen so that the excess carrier density remained low compared to the dopant concentration in the respective silicon samples. Iodine-ethanol [7] has been used for surface passivation of the wafers during the lifetime measurements.

For the comparison between the n- and p-type materials the average diffusion lengths were calculated using the average lifetimes obtained from the lifetime maps. The four-point probe technique (ASTM F43-93, 1996) for resistivity maps was used.

The local recombination activity of extended defects (dislocations and grain boundaries) was studied by Electron Beam Induced Current (EBIC) at room temperature. The EBIC measurements were carried out with a Vega TS5136 XM Tescan Scanning Electron Microscope equipped with an EBIC apparatus. The electron beam excitation was varied from 10 to 30 kV at a beam current kept always below 10 pA. A quantitative analysis of the recombination activity of extended defects was obtained studying the EBIC contrasts ( $C$ ) defined by  $C = (I_b - I_g)/I_b$  where  $I_b$  and  $I_g$  are the EBIC currents in

the bulk and at the GB, respectively. For our set-up, the minimum contrast significantly measurable has been estimated in 0,2% on polished samples.

Before the EBIC measurements, the samples were mechanically and then chemically polished with CP4 (HF:HNO<sub>3</sub>:CH<sub>3</sub>COOH = 3:5:3 in volume ratio). Thereafter, Schottky diodes were realized by evaporating Au or Al on n- and p-type samples respectively.

Some samples were also etched with a *Schimmel* solution (1 g CrO<sub>3</sub>/20 ml HF 48%/10 ml H<sub>2</sub>O) in order to highlight the presence of crystallographic defects, detected and counted both by optical and electron microscopy.

Photoluminescence (PL) spectra at 14 K were recorded with a spectral resolution of 6.6 nm, using an InGaAs detector and a quantum well laser ( $\lambda=805$  nm) as excitation source.

The interstitial oxygen [O]<sub>i</sub> and substitutional carbon [C]<sub>s</sub> content was determined by Fourier Transform InfraRed (FTIR) spectroscopy in the 400-4000 cm<sup>-1</sup> range (ASTM, F1391.93 ; ASTM F1188 93a).

### 3 EXPERIMENTAL RESULTS AND DISCUSSION

#### 3.1 Oxygen and carbon concentration and sample resistivity

Table I reports the results of the oxygen and carbon analysis and the resistivity data for the samples studied in this work. No substantial differences were found between the as-grown and the P-diffused samples.

**Table I** Details (ingot type, dopant and codes) and oxygen, carbon and resistivity data of wafers characterized in this work.

|                       | Ingot 6 (Sb)<br>B2 |         | p-type (B)<br>C1B-B2 |         |
|-----------------------|--------------------|---------|----------------------|---------|
|                       | a.g                | P-diff. | a.g                  | P-diff. |
| Wafer N°              | 245                | 248     | 192                  | 168     |
| [O] (ppma)            | 1.5                |         | 4.5                  |         |
| [C] (ppma)            | 5.5                |         | 5                    |         |
| $\rho$ ( $\Omega$ cm) | 1.5                |         | 1.5                  |         |

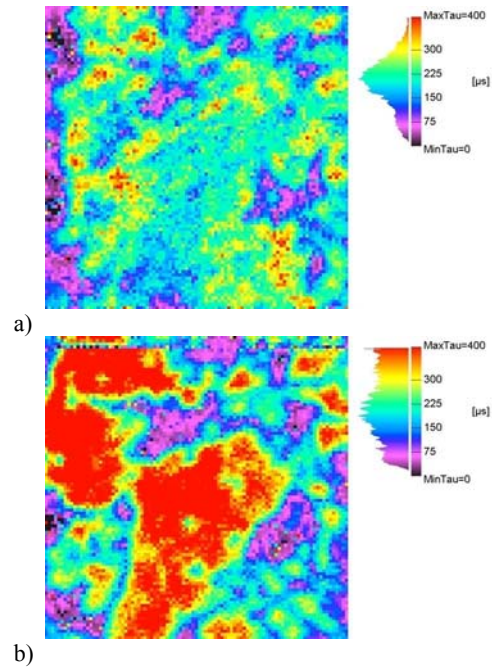
#### 3.2 Lifetime measurements

Figure 1 reports two typical lifetime maps relative to a 5x5 cm<sup>2</sup> section of the Sb-doped wafer before (Figure 1a) and after the POCl<sub>3</sub> process step and the subsequent removal of the doped region (Figure 1b), respectively.

The average lifetime increases after this process due to the well known metallic impurities gettering effect of the P-diffusion [8, 9], but zones of low lifetime are still present. This behaviour has been observed also in the p-type ingot where the overall diffusion length still remains lower respect to the n-type one (see Figure 2).

In order to understand why low lifetime regions remain after the P-diffusion step, we performed a local characterizations of such regions, labelled in the

following as “bad zones” by room temperature EBIC measurements, see Section 3.4.. For comparison purposes, also samples coming from high lifetime regions and denoted as “good zones” have been analysed by EBIC measurements.



**Figure 1** Lifetime  $\mu$ W-PCD maps of the n-type wafers before (a) and after (b) the POCl<sub>3</sub> process step.

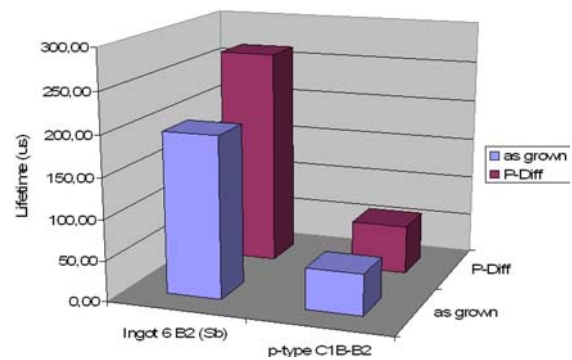


**Figure 2** Average diffusion lengths for the wafers studied obtained from the  $\mu$ W-PCD maps.

#### 3.3 Photoluminescence characterization

In the PL spectra collected in the grain regions the typical peaks associated to the dislocations are present (see Figure 3). The high Free Exciton (FE) emission of the n-type wafers confirms the good quality of the as-grown ingot. Moreover, the effect of P-diffusion detected by PL is essentially related to an increase of the FE intensity, which could be explained by a reduction of metallic contamination by P-gettering.

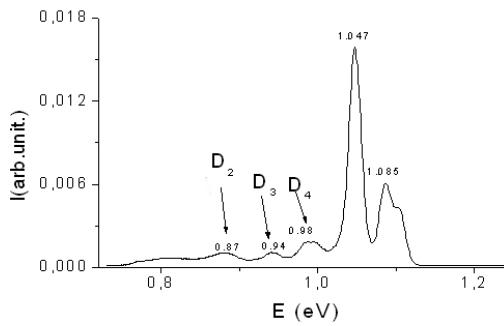


**Figure 3:** Typical PL spectrum collected in a “good zone” of the sample ??? (T= 12 K, power density: 6 W/cm<sup>2</sup>, spot size 1 mm<sup>2</sup>). The dislocation related bands are indicated with the classic notations [D1 (0.8 eV), D2 (0.87 eV), D3 (0.94) D4(0.99 eV)] .

### 3.4 Electron beam induced current (EBIC) measurements

Figure 4a reports a typical EBIC map collected in a “bad zone” of an as-grown sample of the Sb-doped ingot. Electrically active grain boundaries are clearly visible, where the EBIC contrast might be measured.

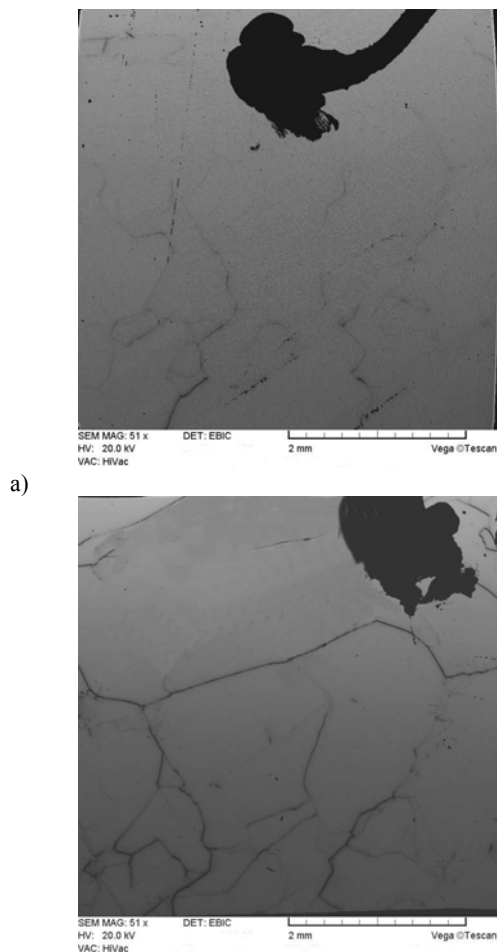


**Figure 4** EBIC maps of the grain boundaries rich zone of the Sb doped ingot before (a) and after (b) the POCl<sub>3</sub> process step.

A low density of active grain boundaries was detected in the good zones. In these last, in the as-grown samples (n-type and p-type), the EBIC GB contrast rarely exceeds 10%. Higher values, of the order of 20-40%, have been detected instead in the “bad zones”.

After the POCl<sub>3</sub> process (Figure 4b) a significant increase in the contrasts was observed for the same defects displayed in Figure 4a. The inhomogeneity of the grain boundary EBIC contrast observed in the different examined samples shows however that the segregation of impurities at defects is not uniform and probably associated to the presence of nanoprecipitates [10]. Another important conclusion suggested by the EBIC analysis is that dislocations, whose presence is revealed by the optical micrograph of a zone previously analysed with EBIC and then submitted to an etching with *Schimmel* solution (Figure 5a and 5b), are electrically inactive. In figure 4b the increased activity of grain boundaries, is, in fact, evident, while no dislocation activity might be detected. From the same Figure it is also evident that a reduction of the activity for some low angle defects (twin grain boundaries) instead occurs.

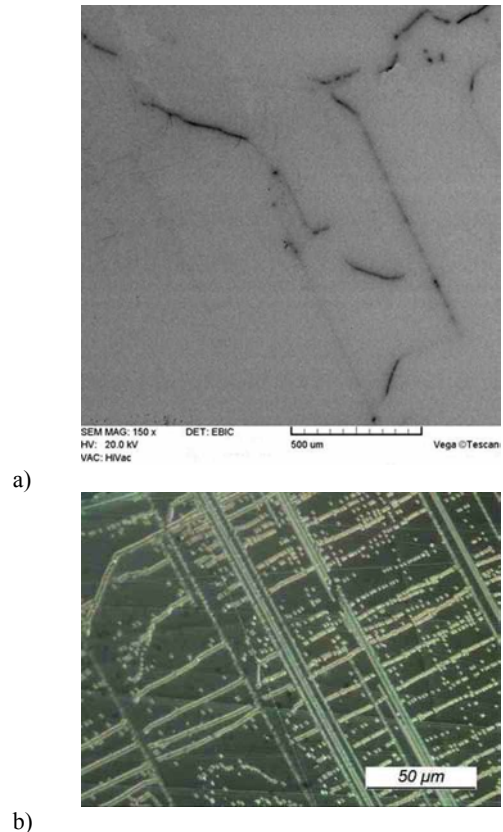
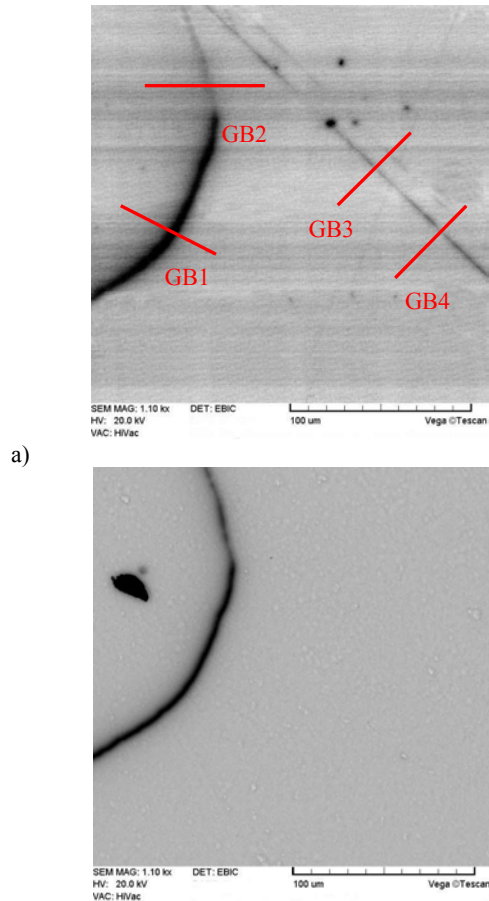


**Figure 5** EBIC map (a) and optical micrograph (b) of a limited zone of the n-type wafer after POCl<sub>3</sub> process. The optical micrograph was obtained after etching the sample with a *Schimmel* solution.

The same behavior was observed for the p-type material, where grain boundaries of low electrical activity were found.

We have therefore demonstrated that an internal gettering process occurs. The question now is whether it is a purely thermal effect occurring during the P-diffusion process and whether it can be controlled and

possibly avoided. Preliminary measurements carried out on the n-type material have shown an increase of local electrical activity of GBs after a thermal annealing at 850 °C for 30 min in air (Figure 6).



a)  
b)  
**Figure 6** EBIC maps of a samples (n-type) before a) and after b) the heat treatment at 850 °C for 30 min.

**Table II** EBIC contrast of the GBs shown in Figure 6.

| Point | Before | After |
|-------|--------|-------|
| GB1   | 0.167  | 0.333 |
| GB2   | 0.053  | 0.333 |
| Gb3   | 0.053  | N.D.* |
| GB4   | 0.053  | N.D.  |

\* N.D. = Non detectable

In Figure 6a are displayed four GB segments were the EBIC contrast was measured before and after the heat treatment. The results are reported in Table II. It is quite evident an increase of the electrical activity of the grain boundaries denoted with GB1 and GB2 while the activity of the twins (GB3 and GB4) is reduced.

#### 4 CONCLUSIONS

We have shown that no substantial difference exists in the beneficial effect of the P-diffusion on p-type and n-type mc-Si. EBIC analyses have however shown that the gettering process of impurities (presumably metallic impurities [10]) is partially suppressed by the presence of

grain boundaries. Several GBs EBIC contrast maps show, in fact, an evident increase of their local electrical activity, which is due to the segregation of impurities after P-diffusion. The efficiency of the internal gettering depends on the GBs structure as already demonstrated by Chen et al. [11]. We have also shown that the same internal gettering effects could be induced by a thermal treatment at 850°C for 30 min in air.

These results might be useful for a future optimization of the solar cell process, which will require a particular attention to the determination of the optimal annealing temperature and duration conditions. Furthermore, despite the formation of precipitates around GBs and their induced electrical activity, we have confirmed that the overall quality of n-type mc-Si is high, possibly greater than that of p-type samples [12], confirming that n-type-Si rejects are a valid resource for photovoltaic application.

#### ACKNOWLEDGEMENTS

This work was supported by the European Commission within the NESSI (contract n° ENK6-CT2002-00660) and the FOXY projects (contract n° 019811).

#### REFERENCES

- [1] R.M. Swanson Prog. Photovolt:Res. Appl. 14 2006 443-453
- [2] J. Libal, T. Buck, R. Kopecek, P. Fath, B. Geerligs, K. Wambach, M. Acciarri, S. Binetti 19<sup>th</sup> EPSEC, Palais des Congrès, Paris, France, 7-11 June 2004
- [3] R. Kopecek, J. Libal, T. Buck, K. Peter, K. Wambach, M. Acciarri, S. Binetti, L.J. Geerligs, P. Fath, Conference Record of the 31<sup>st</sup> IEEE Photovoltaic Specialists Conference (2005)
- [4] T. Buck, R. Kopecek, J. Libal, R. Petres, K. Peter, I. Röver, K. Wambach, L.J. Geerligs, E. Wefringhaus, P. Fath 4<sup>th</sup> World Conference on Photovoltaic Energy Conversion- May 7-12, 2006 Waikoloa, Hawaii, USA
- [5] L.J. Geerligs, C.J.J. Tool, R. Kinderman, I. Röver, K. Wambach, R. Kopecek, T. Buck, J. Libal, R. Petres, P. Fath, P. Sánchez-Friera, J. Alonso, M. Acciarri, S. Binetti, S. Pizzini. This conference.
- [6] F. Ferrazza et al. Proceedings of the 2<sup>nd</sup> Word Conference and Exhibition on Photovoltaic Solar Energy Conversion, 1998 Vienna (Austria).
- [7] T.S. Horányi, T. Pavelka, T. Tüttö, Appl. Surf. Sci. 63 (1993) 306
- [8] Perichaud, Solar Energy Materials and Solar Cells 72 (2002) 315
- [9] A. Cuevas, M. Stocks, S. Armand, M. Stuckings, A. Blakers, F. Ferrazza, Appl. Phys.Lett. 70 (1997) 1017
- [10] A.A. Istratov, T. Buonassisi, R.J. McDonald, A.R. Smith, R. Schinder, J.A. Rand, J.P. Kalejs, E.R. Weber, J.Appl.Phys. 94 (2003) 6552
- [11] J. Chen, T. Sekiguci, D. Yang, F. yin, K. Kido, S. Tsurekawa, J.Appl.Phys. 96 (2004) 5490
- [12] L.J. Geerligs, D.Macdonald, Prog. Photovolt: Res. Appl. 12 (2004) 309